

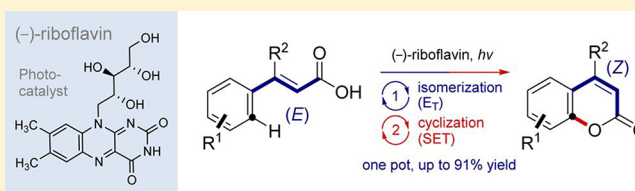
One Photocatalyst, n Activation Modes Strategy for Cascade Catalysis: Emulating Coumarin Biosynthesis with (–)-Riboflavin

Jan B. Metternich and Ryan Gilmour*

Institute for Organic Chemistry, Westfälische Wilhelms-Universität Münster, Corrensstrasse 40, 48149 Münster, Germany

S Supporting Information

ABSTRACT: Generating molecular complexity using a single catalyst, where the requisite activation modes are sequentially exploited as the reaction proceeds, is an attractive guiding principle in synthesis. This requires that each substrate transposition exposes a catalyst activation mode (AM) to which all preceding or future intermediates are resistant. While this concept is exemplified by MacMillan's beautiful merger of enamine and iminium ion activation, examples in other fields of contemporary catalysis remain elusive. Herein, we extend this tactic to organic photochemistry. By harnessing the two discrete photochemical activation modes of (–)-riboflavin, it is possible to sequentially induce isomerization and cyclization by energy transfer (E_T) and single-electron transfer (SET) activation pathways, respectively. This catalytic approach has been utilized to emulate the coumarin biosynthesis pathway, which features a key photochemical $E \rightarrow Z$ isomerization step. Since the ensuing SET-based cyclization eliminates the need for a prefunctionalized aryl ring, this constitutes a novel disconnection of a pharmaceutically important scaffold.



INTRODUCTION

Orchestrating multiple activation modes of a single catalyst to perform sequential transformations on a specific precursor is an attractive guiding principle in generating molecular complexity.¹ To be effective, this necessarily requires that each substrate transposition exposes a catalyst activation mode to which all preceding or future intermediates are resistant. Consequently, this strategy installs an intrinsic directionality to the overall catalytic sequence, thus conserving selectivity.² The efficiency of what is formally cascade catalysis using a single catalyst is exemplified by MacMillan's seminal merger of iminium and enamine activation modes using a low-molecular-weight imidazolidinone.³ This unification of two discrete catalytic cycles to generate multiple bonds in a highly stereoselective manner is a compelling endorsement for the development of this approach in contemporary catalysis. Conceptually, this notion may be considered antipodal to the established fields of synergistic (n catalysts \rightarrow 1 product)⁴ or divergent (n catalysts \rightarrow n products, $n > 1$) catalysis,⁵ both of which also begin with a common precursor (Figure 1). Inspired by these and other conceptually related examples employing multiple catalysts,⁶ changes in reaction conditions,⁷ or a heterogeneous platform,⁸ efforts to translate this concept from the realm of covalent organocatalysis to noncovalent photocatalysis⁹ were initiated; this seemed judicious on account of the multiple activation modes (AM) that are inherent to the majority of common photocatalysts.¹⁰

For this preliminary validation, an intramolecular cascade was sought to simplify any subsequent mechanistic analyses. Translating the biosynthesis of coumarin into a small molecule catalysis paradigm was selected as the benchmark trans-

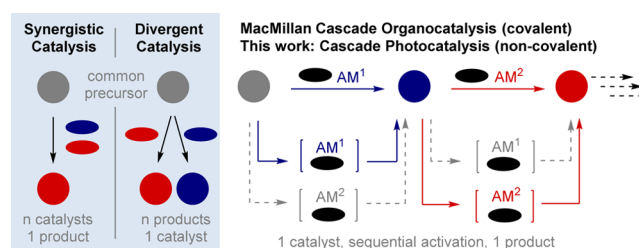


Figure 1. Overview of the one catalyst, n activation modes strategy and conceptual comparison with synergistic and divergent catalyses. AM = activation mode.

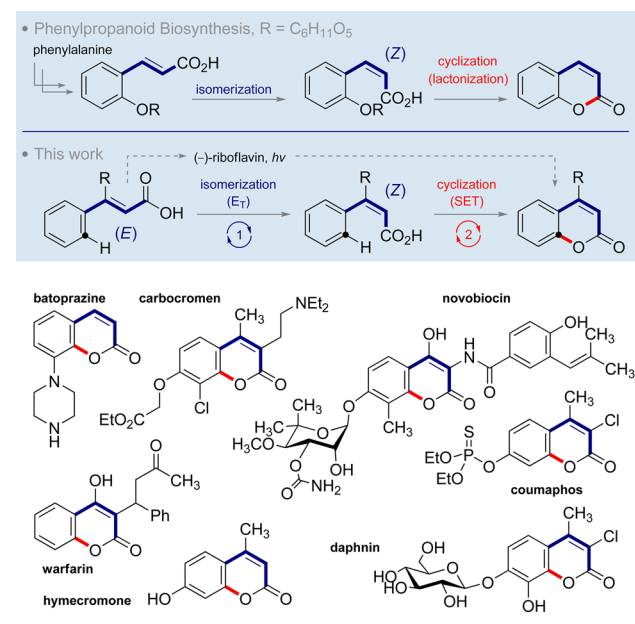
formation (Scheme 1, upper). This would require sequential engagement of the energy transfer and single-electron transfer (SET) activation modes of the inexpensive photocatalyst (–)-riboflavin.¹¹ By correlating structure to activation mode, a one-step conversion of simple E -cinnamic acids to this privileged drug scaffold was envisaged.¹²

A striking manifestation of nature's conversion of light into chemical energy is the pivotal $E \rightarrow Z$ photoisomerization in coumarin biosynthesis.¹³ Originating from phenylalanine via the phenylpropanoid pathway, the biosynthesis of the 1,2-benzopyrone scaffold is characterized by a postulated cytochrome P450-mediated $C(sp^2)$ oxidation, followed by an isomerization–glycolysis–lactonization sequence (Scheme 1, upper).¹⁴ Given the frequency with which this structural element appears in biology, it is perhaps unsurprising that it has a distinguished lineage in pharmaceutical development and

Received: November 24, 2015

Published: December 30, 2015

Scheme 1. (Upper) Biosynthesis of the Coumarin Scaffold and the Envisaged Photocatalytic Strategy Employing (–)-Riboflavin and (Lower) Bioactive Natural Products Containing a Coumarin Core



constitutes the core of numerous natural products.¹⁵ Pertinent examples include the natural and non-natural therapeutics, novobiocin and warfarin, respectively (Scheme 1, lower). Unsurprisingly, the ubiquity of coumarins in therapeutic medicine and chemical biology has stimulated the development of numerous synthetic strategies, most of which rely on lactone formation as the key step.¹⁶ However, these approaches require prefunctionalized aryl moieties prior to cyclization, which often erodes step economy. To complement existing methodology, efforts to devise a bioinspired, catalysis-based route were investigated.

Herein, we report a concise, one-pot strategy that does not rely on a phenol-derived starting material but instead utilizes simple (*E*)-cinnamic acids. It was envisaged that the need for a prefunctionalized aryl ring could be surpassed by employing (–)-riboflavin as a photocatalyst, thereby sequentially exploiting the energy transfer (E_T)¹⁷ based olefin isomerization, with concomitant cyclization facilitated by SET catalysis.¹⁸ Engaging the two activation modes of (–)-riboflavin would thereby allow the biogenetic route to the coumarin nucleus to be emulated while providing a novel disconnection of this important core using simple starting materials (highlighted in red, Scheme 1).¹⁹

RESULTS

To evaluate this hypothesis, a representative (*E*)-cinnamic acid was independently dissolved in various polar solvent combinations and exposed to UV irradiation (402 nm; for full characterization of the UV light source, see the Supporting Information, page S2) in the presence of 5 mol % photocatalyst (Table 1, catalyst a). This optimization process quickly revealed MeCN/MeOH (1:1) to be the reaction medium of choice,^{17b} with molecular oxygen proving to be a clean and effective oxidant.¹⁹ Investigation of the effect of olefin geometry (*E*/*Z*) and comparison of (–)-riboflavin (a) with 3-methylumiflavin (b) completed this process and gave rise to a set of standard conditions by which coumarin formation proved to be efficient

Table 1. Reaction Optimization^a

substrate geometry	catalyst (5 mol %)	solvent	yield [%]
E	a	MeCN	30 ^b
E	a	MeOH	37 ^b
E	a	DMSO	<10 ^b
E	a	MeCN/MeOH (1:1)	61 ^b
E	a	MeCN/MeOH (9:1)	51 ^b
E	a	MeCN/MeOH (7.5:2.5)	46 ^b
E	a	MeCN/EtOAc (1:1)	37 ^b
E	a	MeCN/H ₂ O (1:1)	41 ^b
E	a	MeCN/HFIP (1:1)	<30 ^b
E	b	MeCN/MeOH (1:1)	36 ^c
Z	a	MeCN/MeOH (1:1)	90
E	a ^d	MeCN/MeOH (1:1)	90

^aStandard reactions conditions: reactions were performed with 0.1 mmol substrate (*E*/*Z* > 20:1) at ambient temperature under 24 h of UV-light irradiation (402 nm) and an oxygen atmosphere. (–)-Riboflavin is commercially available from Sigma-Aldrich (CAS 83-88-5). ^bSignificant remaining *Z* isomer detected on TLC. ^cSignificant remaining *E* isomer detected on TLC. ^dAddition of a second portion (5 mol %) of the catalyst after 12 h.

(90% yield). To address the well-documented propensity of (–)-riboflavin to undergo photodegradation following prolonged exposure to UV light,²⁰ a second batch of photocatalyst (5 mol %) was added to the reaction after 12 h; this ensured that the ensuing cyclization step was not impeded.

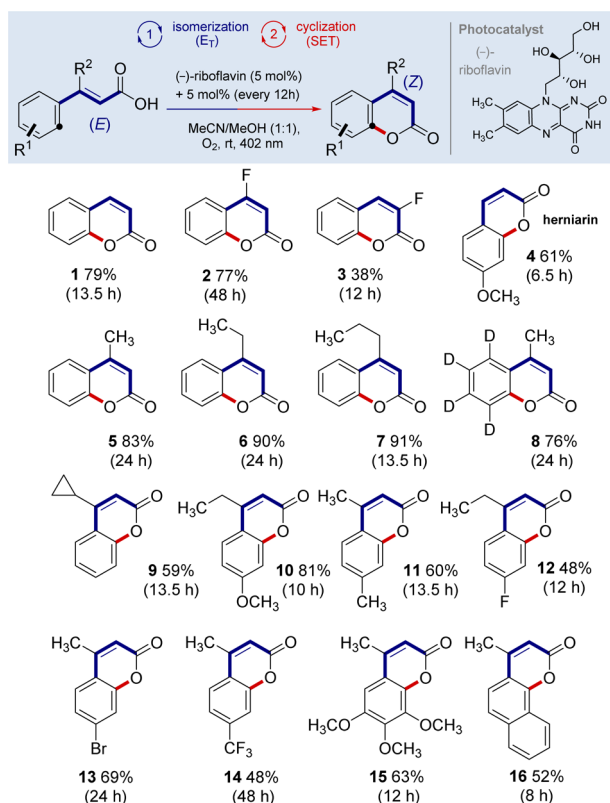
Having devised a catalysis protocol, the scope and limitations of the transformation were investigated with a range of structurally and electronically modulated substrates (Scheme 2). In view of the importance of fluorine incorporation in drug discovery,²¹ the influence of bioisosteric H to F substitution at the α - and β -positions of the starting cinnamic acids was first examined. In both cases, the expected fluorinated coumarins were isolated in 77 and 38% yields (2 and 3, respectively).

Next, validation of the method in the synthesis of the natural product herniarin (4) was performed. Exposure of *p*-methoxy cinnamic acid to the optimized photocatalysis condition furnished target molecule 4 in 61% yield after 6.5 h; this provides a complementary route to those used in current state-of-the-art strategies.²²

Systematically augmenting the β substituent from CH₃ (5) to C₂H₅ (6), and C₃H₇ (7) led to enhanced reaction yields [83, 90, and 91%, respectively; cf. 79% for H (1)]. This observation can be rationalized by the radical stabilizing effect of the substituent during the initial isomerization step.^{17b} Deuterated analogue 8 was included in this study (76%) with a view toward probing the mechanism in a later kinetic analysis. To explore the notion of an intermediary radical species, the cyclopropyl derivative was exposed to the standard photocatalysis conditions. The expectation that formation of 9 would compete with radical-induced ring opening was reflected in a slightly lower yield (59%).

Substituents on the aryl ring were generally well-tolerated, as exemplified by the series 10 (OMe), 11 (Me), and 12 (F): 81, 60, and 48% yields, respectively. Interestingly, the lower yield of

Scheme 2. Scope and Limitations of the Photocatalysis Route to Coumarins Catalyzed by (–)-Riboflavin^a



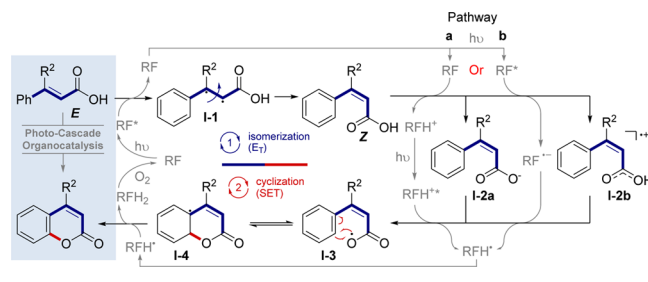
^aStandard reaction conditions: reactions were performed under oxygen atmosphere with 0.1 mmol substrate (*E/Z* > 20:1) at ambient temperature in MeCN/MeOH using 5 mol % catalyst loading. An additional 5 mol % catalyst was added every 12 h. The specified time of UV-light irradiation (402 nm) is given in parentheses.

7-fluorine-substituted coumarin **12** can be attributed to a competing photochemical C–F bond activation²³ and subsequent trapping with MeOH to yield **10** as a side product. In view of the importance of aryl bromides in cross-coupling transformations, coumarin **13** was prepared to demonstrate functional group tolerance (69% yield). Trifluoromethylated derivative **14** could also be accessed under the standard conditions, albeit with a slight reduction in yield (48%). Highly activated systems, such as trimethoxy derivative **15**, were also well-tolerated (63%, 12 h). Furthermore, naphthyl-derived coumarin **16**, a common precursor in the synthesis of various naphthopyran-2-ones,²⁴ was formed regioselectively starting from 3-(naphthalenyl)-but-2-enoic acid (**16**, 52%). In this particular case, the reaction time had to be significantly reduced (to 8 h) due to the high UV sensitivity of the product, which itself can function as a photosensitizer.²⁵

DISCUSSION

Since the reaction proceeds efficiently, irrespective of the starting *E/Z* olefin geometry, a single-step mechanism can reasonably be discounted. Thus, a tentative hypothesis based on two distinct photocatalyst activation modes was envisaged (Scheme 3). Previously, this laboratory has reported that (–)-riboflavin efficiently catalyzes the *E* → *Z* isomerization of activated olefins embedded within the cinnamaldehyde substructure.^{17b} A mechanism consistent with selective triplet state energy transfer (*E_T*) to the *E* isomer generates intermediate **I-1**

Scheme 3. Tentative Mechanistic Proposal



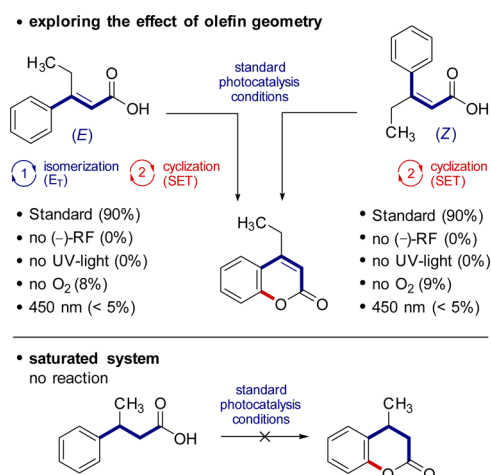
possessing biradical character: this has been corroborated by stereomutation experiments. Following this initial selective excitation, all ensuing processes are energetically downhill and can give rise to either the *E* or *Z* isomer. Stereoselectivity arises from the differing photophysical properties of the reactant and product isomers: the *Z* isomer is not re-excited by energy transfer as a consequence of deconjugation of the now twisted π -system (*A*^{1,3}-strain) in the product, resulting in significantly increased triplet state energies.²⁶

This postulation is accompanied by the caveat that an energy transfer process can be excluded from the ensuing cyclization. It seemed likely that a SET process was operational in the second step of the coumarin formation.

Interestingly, a SET process catalyzed by (–)-riboflavin can occur via two discrete pathways: (a) deprotonation of the carboxylic acid **Z** by (–)-riboflavin, yielding **I-2a**, with subsequent excitation at 402 nm resulting in the abstraction of an electron,²⁷ or (b) excitation of (–)-riboflavin, resulting in electron abstraction to generate intermediate **I-2b** followed by deprotonation.¹⁹ Independent of the activation pathway, radical intermediate **I-3** is ultimately formed, which can undergo cyclization to intermediate **I-4**. In the final step, formal abstraction of a hydrogen atom by riboflavin in an H atom transfer or SET/deprotonation step yields the target coumarin and liberates reduced RFH₂; this is subsequently oxidized by O₂ to generate (–)-riboflavin, thus closing the catalytic cycle. In an effort to further delineate the mechanism, a series of control experiments was performed (Scheme 4).

Initially, both geometric isomers *E*- and *Z*-**21** were independently submitted to the standard photocatalytic conditions. These conditions were then successively modified, and the resulting yields were compared to those recorded under the standard conditions. As expected, both stages of the reaction require UV irradiation and (–)-riboflavin as a catalyst (ca. 90% yield). Performing the reaction in the absence of oxygen using degassed solvents led to drastic drops in yield (8 and 9% for the *E* and *Z* isomers, respectively), supporting the notion that O₂ is the terminal oxidant. The marginal deviation of these yields from the initial catalyst loading (5 mol %) can be attributed to residual oxygen in the reaction media. Nonetheless, these data support the notion that the reduced riboflavin formed during the reaction is subsequently oxidized by atmospheric O₂.

To further support the involvement of protonated (–)-riboflavin (pathway a) in the stage preceding cyclization, the reaction was performed at 450 nm (for full characterization of the UV light source, see the Supporting Information, page S3); this corresponds to the second absorption maximum of the photocatalyst. An absorption shift to 402 nm is expected upon protonation of (–)-riboflavin.²⁸ Under these conditions, only trace amounts of product were formed (<5%), further

Scheme 4. Control Experiments To Support the Mechanistic Hypothesis⁴

“Standard reaction conditions: reactions were performed under an oxygen atmosphere with 0.1 mmol substrate at ambient temperature in MeCN/MeOH using 5 mol % catalyst loading. An additional 5 mol % catalyst was added every 12 h.

strengthening this hypothesis. Although it was not possible to validate this spectroscopically using the substrate due to limited solubility, the absorption shift to 402 nm is clearly visible when adding TFA to a solution of (-)-riboflavin in $H_2O/MeCN$ (Figure 2).

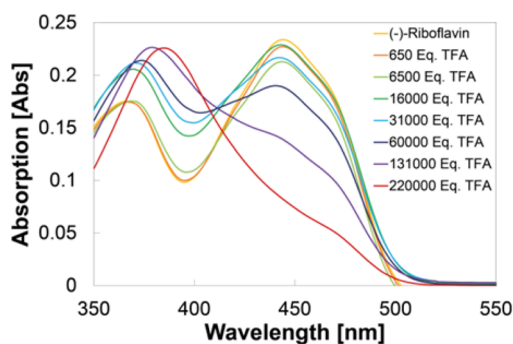


Figure 2. Effect of TFA on the absorption of (-)-riboflavin. Measurements were performed in $H_2O/MeCN$ (1:1).

The saturated analogue 3-phenylbutanoic acid (Scheme 4, lower) was submitted to the standard reaction conditions to demonstrate the requirement of an olefin moiety in this transformation. No product formation was observed, validating the importance of the conjugated system.

The isomerization and cyclization stages of the process were then monitored over a period of 24 h using an electron-rich (*E*- and *Z*-21; Figure 3a,b) and an electron-deficient olefin pair (*E*- and *Z*-29; Figure 3c,d). For all systems, complete *Z*-selective isomerization was observed over the course of 3 h. This formation and accumulation of a stable, isolable reaction intermediate is in line with the proposal that two different mechanisms are operating in concert. Moreover, the slow consumption of the intermediate *Z* isomer suggests that the cyclization is the overall rate-determining step. In both cases starting from the *E* isomer (Figure 3a,c), a short induction period of ca. 1 h was recorded during which coumarin formation was not observed. This induction phase suggests that

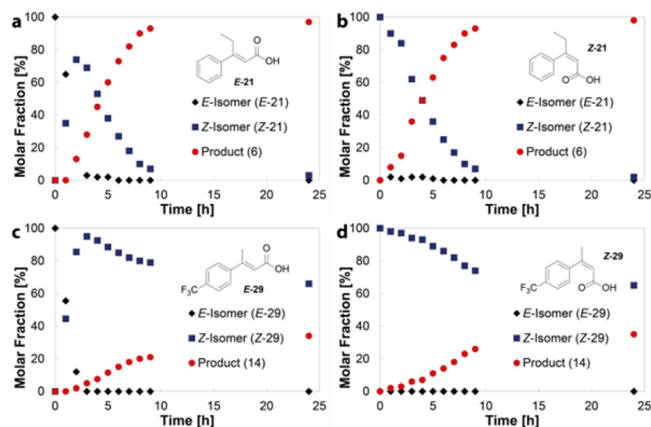


Figure 3. Reaction progress monitoring starting from the *E* and *Z* isomers of two model substrates: (a) *E*-21, (b) *Z*-21, (c) *E*-29, and (d) *Z*-29.

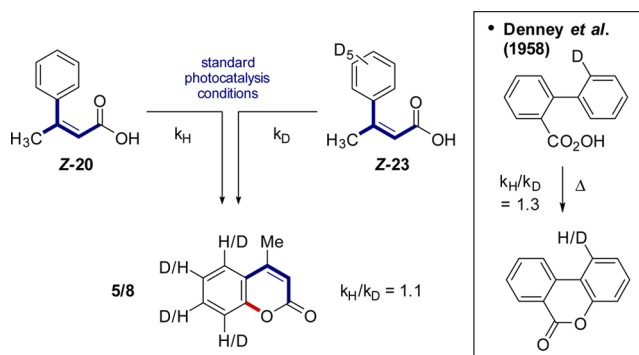
the cyclization is linked to a second mechanism starting from the *Z* isomer.

Direct comparison of reactions starting from the *E* or *Z* isomer proved to be instructive. In the case of the substrates *E*- and *Z*-21 (*p*-H, β -Et; Figure 3a,b, respectively), product formation reached a common percentage after 7 h, independent of the olefin geometry. The resulting conversions to the coumarin were 93 and 97%, after 9 and 24 h, respectively.

That the cyclization is rate-determining is significantly more pronounced in the deactivated substrate pair (*E*- and *Z*-29; *p*- CF_3 , β -Me; Figure 3c,d, respectively). Despite the isomerization reaching completion after only 3 h, the cyclization required extended reaction times and the rate of product formation further decreased after reaching approximately 30% conversion. This erosion of the reaction rate can be explained by in situ quenching of the excited state of (-)-riboflavin by the product, thus impacting the overall yield.

To probe the final cyclization step, a kinetic isotope effect and additive study was performed (Scheme 5). Reactions of the

Scheme 5. Kinetic Isotope Effect Study



nondeuterated and deuterated *Z* isomers (*Z*-20 and *Z*-23) were monitored, and the region of linear reaction progress between 0 and 5 h was compared. As a result, a kinetic isotope effect of 1.1 was measured; this is consistent with a report from Denney *et al.*²⁹ for an analogous, thermally induced cyclization of the 2-(2-deuteriophenyl)-benzoylperoxide system ($k_H/k_D = 1.3$; Scheme 5, right). On the basis of literature precedent, it is plausible that the attack of the benzoyl radical is reversible; consequently, one

of the SET processes is likely the rate-determining step of the cyclization.³⁰

Finally, the effect of acidic (TFA) or basic (NaOMe) additives was investigated (Figure 4). Whereas the addition of 1

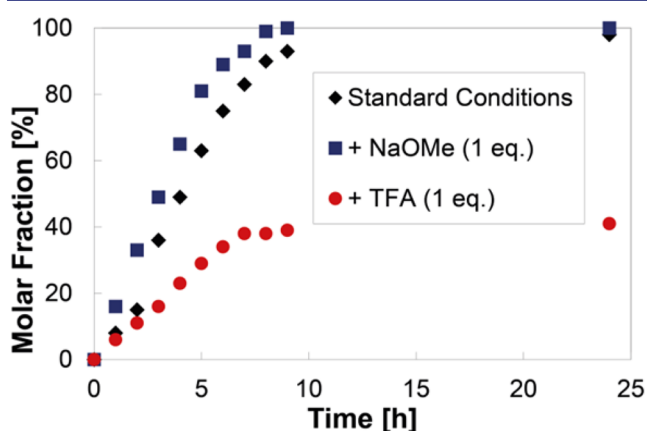


Figure 4. Reaction progress monitoring to probe the effect of acidic and basic additives on the conversion of the Z isomer (Z-21) to the corresponding coumarin 6.

equivalent of NaOMe results in an increase in rate due to deprotonation of cinnamic acid prior to excitation, the addition of an equimolar quantity of TFA significantly retards the process. Since carboxylate anions are known for rapid electron transfer in interaction with an excited electron acceptor, deprotonation likely increases the reaction rate; this process is inhibited by addition of TFA.³¹

An increase in the reaction rate under basic conditions may indicate that excitation is occurring via pathway **b** (Scheme 3) because (–)-riboflavin [pK_a (RFH⁺ = 0.25)]^{28c} will be deprotonated in the presence of NaOMe. Because neither extreme is representative of the standard reaction conditions, neither pathway can be entirely excluded.

CONCLUSIONS

The concept of sequentially engaging multiple activation modes of a single catalyst to generate molecular complexity has been translated to the paradigm of noncovalent (photocascade) catalysis and benchmarked in a direct synthesis of coumarins from *E*-cinnamic acids. This biomimetic strategy does not require prefunctionalization of the aryl ring prior to cyclization and thus constitutes a novel disconnection of these pharmaceutically important compounds. Conceptually, this work complements established one catalyst, two reaction approaches in that it does not require a change in conditions and that simple substrate transpositions stimulate contrasting catalysis behaviors. Through a combination of control experiments, progress monitoring experiments, and kinetic isotope studies, it has been possible to validate the initial mechanistic hypothesis that merges energy transfer (E_T) and subsequent SET processes. In view of the current interest in organic photocatalysis and the wealth of information pertaining to light-induced activation modes, it is envisaged that this guiding principle will evolve to complement the antipodal field of synergistic catalysis.

ASSOCIATED CONTENT

Supporting Information

The Supporting Information is available free of charge on the ACS Publications website at DOI: 10.1021/jacs.5b12081.

NMR spectra, absorption spectra, experimental procedures, and mechanistic studies (PDF)

AUTHOR INFORMATION

Corresponding Author

*ryan.gilmour@uni-muenster.de

Notes

The authors declare no competing financial interest.

ACKNOWLEDGMENTS

We acknowledge generous financial support from the WWU Münster, the Deutsche Forschungsgemeinschaft (SFB 858 and Excellence Cluster EXC 1003 “Cells in Motion – Cluster of Excellence”), and the Fonds der Chemischen Industrie (FCI Fellowship to J. B. Metternich). This study is dedicated to Prof. Dr. Steven V. Ley FRS on the occasion of his 70th birthday.

REFERENCES

- (1) (a) Wender, P. A. *Nat. Prod. Rep.* **2014**, *31*, 433–440. (b) Wender, P. A.; Miller, B. L. *Nature* **2009**, *460*, 197–201. (c) Trost, B. M. *Science* **1991**, *254*, 1471–1477.
- (2) Walji, A. M.; MacMillan, D. W. C. *Synlett* **2007**, *2007*, 1477–1489.
- (3) (a) Austin, J. F.; Kim, S. G.; Sinz, C. J.; Xiao, W. J.; MacMillan, D. W. C. *Proc. Natl. Acad. Sci. U. S. A.* **2004**, *101*, 5482–5487. (b) Huang, Y.; Walji, A. M.; Larsen, C. H.; MacMillan, D. W. C. *J. Am. Chem. Soc.* **2005**, *127*, 15051–15053. For an example of enantioselective organo-SOMO cascade cycloadditions, see (c) Jui, N. T.; Lee, E. C. Y.; MacMillan, D. W. C. *J. Am. Chem. Soc.* **2010**, *132*, 10015–10017.
- (4) For a review of synergistic catalysis, see Allen, A. E.; MacMillan, D. W. C. *Chem. Sci.* **2012**, *3*, 633–658.
- (5) For seminal examples of stereodivergent dual catalysis, see (a) Krautwald, S.; Sarlah, D.; Schafoth, M. A.; Carreira, E. M. *Science* **2013**, *340*, 1065–1068. (b) Krautwald, S.; Schafoth, M. A.; Sarlah, D.; Carreira, E. M. *J. Am. Chem. Soc.* **2014**, *136*, 3020–3023. For a recent perspective, see (c) Schindler, C. S.; Jacobsen, E. N. *Science* **2013**, *340*, 1052–1053.
- (6) For a recent discussion of orthogonal tandem catalysis, see Lohr, T. L.; Marks, T. J. *Nat. Chem.* **2015**, *7*, 477–482.
- (7) Shi, S.-L.; Buchwald, S. L. *Nat. Chem.* **2014**, *7*, 38–44.
- (8) Yamada, Y.; Tsung, C.-K.; Huang, W.; Huo, Z.; Habas, S. E.; Soejima, T.; Aliaga, C. E.; Somorjai, G. A.; Yang, P. *Nat. Chem.* **2011**, *3*, 372–376.
- (9) (a) Lin, Q.-Y.; Xu, X.-H.; Qing, F.-L. *J. Org. Chem.* **2014**, *79*, 10434–10446. For recent reviews on organic photocatalysis, see (b) Yoon, T. P.; Ischay, M. A.; Du, J. *Nat. Chem.* **2010**, *2*, 527–532. (c) Narayanam, J. M. R.; Stephenson, C. R. J. *Chem. Soc. Rev.* **2011**, *40*, 102–113. (d) Xuan, J.; Xiao, W. *Angew. Chem., Int. Ed.* **2012**, *51*, 6828–6838; (e) *Angew. Chem.* **2012**, *124*, 6934–6944. (f) Prier, C. K.; Rankic, D. A.; MacMillan, D. W. C. *Chem. Rev.* **2013**, *113*, 5322–53263. (g) Koike, T.; Akita, M. *Synlett* **2013**, *24*, 2492–2505. (h) Yoon, T. P.; Stephenson, C. R. J. *Adv. Synth. Catal.* **2014**, *356*, 2739–2739. (i) Schultz, D. M.; Yoon, T. P. *Science* **2014**, *343*, 1239176. (j) Nicewicz, D. A.; Nguyen, T. M. *ACS Catal.* **2014**, *4*, 355–360. (k) Brimiouille, R.; Lenhart, D.; Maturi, M. M.; Bach, T. *Angew. Chem., Int. Ed.* **2015**, *54*, 3872–3890; (l) *Angew. Chem.* **2015**, *127*, 3944–3963.
- (10) Turro, N. J.; Ramamurthy, V.; Scaiano, J. C. *Modern Molecular Photochemistry of Organic Molecules*; University Science Books: Sausalito, CA, 2010.
- (11) Massey, V. *Biochem. Soc. Trans.* **2000**, *28*, 283–296.

- (12) Peng, X. M.; Damu, G. L.; Zhou, C. *Curr. Pharm. Des.* **2013**, *19*, 3884–3930.
- (13) Edwards, K. G.; Stoker, J. R. *Phytochemistry* **1967**, *6*, 655–661.
- (14) Matern, U.; Lüerm, P.; Kreuzsch, D. Biosynthesis of Coumarins. In *Comprehensive Natural Product Chemistry: Polyketides and Other Secondary Metabolites*; Sankawa, U., Ed.; Pergamon, Oxford, 1999; Vol. 1.
- (15) (a) Estévez-Braun, A.; González, A. G. *Nat. Prod. Rep.* **1997**, *14*, 465–475. (b) *Coumarins: Biology, Applications, and Mode of Action*; O’Kennedy, R., Thomas, R. D., Eds.; Wiley: Chichester, UK, 1997.
- (16) Boeck, F.; Blazejak, M.; Anneser, M. R.; Hintermann, L. *Beilstein J. Org. Chem.* **2012**, *8*, 1630–1638 and references cited therein.
- (17) (a) Posthuma, J.; Berends, W. *Biochim. Biophys. Acta* **1960**, *41*, 538–541. (b) Metternich, J. B.; Gilmour, R. *J. Am. Chem. Soc.* **2015**, *137*, 11254–11257.
- (18) (a) Land, E. J.; Swallow, A. J. *Biochemistry* **1969**, *8*, 2117–2125. (b) Surdhar, P. S.; Armstrong, D. *Int. J. Radiat. Biol.* **1987**, *52*, 419–435. (c) Fukuzumi, S.; Kuroda, S.; Tanaka, T. *J. Am. Chem. Soc.* **1985**, *107*, 3020–3027. (d) Murahashi, S.; Oda, T.; Masui, Y. *J. Am. Chem. Soc.* **1989**, *111*, 5002–5003. (e) Martin, C. B.; Tsao, M.-L.; Hadad, C. M.; Platz, M. S. *J. Am. Chem. Soc.* **2002**, *124*, 7226–7234. (f) Imada, Y.; Iida, H.; Ono, S.; Murahashi, S.-I. *J. Am. Chem. Soc.* **2003**, *125*, 2868–2869. (g) Megerle, U.; Wenninger, M.; Kutta, R.-J.; Lechner, R.; König, B.; Dick, B.; Riedle, E. *Phys. Chem. Chem. Phys.* **2011**, *13*, 8869–8880. (h) Dadova, J.; Kümmel, S.; Feldmeier, C.; Cibulkova, J.; Pazout, R.; Maixner, J.; Gschwind, R. M.; König, B.; Cibulka, R. *Chem. - Eur. J.* **2013**, *19*, 1066–1075. (i) Feldmeier, C.; Bartling, H.; Magerl, K.; Gschwind, R. M. *Angew. Chem., Int. Ed.* **2015**, *54*, 1347–1351; *Angew. Chem.* **2015**, *127*, 1363–1367.
- (19) For a discussion of the reaction of carboxylic acid anions with (–)-riboflavin, see (a) Heelis, P. F. *Chem. Soc. Rev.* **1982**, *11*, 15–39. For a recent catalytic, dehydrogenative lactonization of 2-arylbenzoic acids to benzocoumarins invoking this intermediate, see (b) Ramirez, N. P.; Bosque, I.; Gonzalez-Gomez, J. C. *Org. Lett.* **2015**, *17*, 4550–4553.
- (20) (a) Smith, E. C.; Metzler, D. E. *J. Am. Chem. Soc.* **1963**, *85*, 3285–3288. (b) Wadke, D. A.; Guttman, D. E. *J. Pharm. Sci.* **1966**, *55*, 1363–1368. (c) de La Rochette, A.; Silva, E.; Birlouez-Aragon, I.; Mancini, M.; Edwards, A.-M.; Morlière, P. *Photochem. Photobiol.* **2000**, *72*, 815–820. (d) Sheraz, M. A.; Kazi, S. H.; Ahmed, S.; Anwar, Z.; Ahmad, I. *Beilstein J. Org. Chem.* **2014**, *10*, 1999–2012.
- (21) (a) Purser, S.; Moore, P. R.; Swallow, S.; Gouverneur, V. *Chem. Soc. Rev.* **2008**, *37*, 320–330. (b) *Fluorine in Pharmaceutical and Medicinal Chemistry*; Gouverneur, V., Müller, K., Eds.; Imperial College Press: London, 2010.
- (22) For recent examples of coumarin synthesis strategies, see (a) Trost, B. M.; Toste, F. D.; Greenman, K. *J. Am. Chem. Soc.* **2003**, *125*, 4518–4526. (b) Ferguson, J.; Zeng, F.; Alper, H. *Org. Lett.* **2012**, *14*, 5602–5605. (c) Sasano, K.; Takaya, J.; Iwasawa, N. *J. Am. Chem. Soc.* **2013**, *135*, 10954–10957. (d) Zhang, X.-S.; Li, Z.-W.; Shi, Z.-J. *Org. Chem. Front.* **2014**, *1*, 44–49. (e) Medina, F. G.; Marrero, J. G.; Maciás-Alonso, M.; González, M. C.; Córdova-Guerrero, I.; Teissier García, A. G.; Osegueda-Robles, S. *Nat. Prod. Rep.* **2015**, *32*, 1472–1507. (f) Liu, X.-G.; Zhang, S.-S.; Jiang, C.-Y.; Wu, J.-Q.; Li, Q.; Wang, H. *Org. Lett.* **2015**, *17*, 5404–5407. (g) Gadakh, S. K.; Dey, S.; Sudalai, A. *J. Org. Chem.* **2015**, *80*, 11544–11550.
- (23) (a) Senaweera, S. M.; Singh, A.; Weaver, J. D. *J. Am. Chem. Soc.* **2014**, *136*, 3002–3005. (b) Singh, A.; Kubik, J. J.; Weaver, J. D. *Chem. Sci.* **2015**, *6*, 7206–7212. (c) Dewanji, A.; Mück-Lichtenfeld, C.; Bergander, K.; Daniliuc, C. G.; Studer, A. *Chem. - Eur. J.* **2015**, *21*, 12295–12298.
- (24) Saleh, R. M.; Soliman, A. Y.; El Nagdy, S.; Bakeer, H. M.; Mostafa, M. M. *Phosphorus, Sulfur Silicon Relat. Elem.* **1990**, *48*, 285–288.
- (25) (a) Hammond, G. S.; Stout, C. A.; Lamola, A. A. *J. Am. Chem. Soc.* **1964**, *86*, 3103–3106. (b) Hoffman, R.; Wells, P.; Morrison, H. *J. Org. Chem.* **1971**, *36*, 102–108. (c) Winters, B. H.; Mandelberg, H. I.; Mohr, W. B. *Appl. Phys. Lett.* **1974**, *25*, 723–725. (d) von Trebra, R. J.; Koch, T. H. *J. Photochem.* **1986**, *35*, 33–46.
- (26) For a discussion of relevant triplet state energies (E_T) and the corresponding Stern–Volmer quenching plot of the isomerization step using an ethyl ester, see ref 17b. Repeated attempts to perform a Stern–Volmer quenching analysis of the cyclization process failed. It was not possible to generate sufficiently concentrated solutions of the substrate in the aqueous media required to dissolve (–)-riboflavin.
- (27) Fukuzumi, S.; Tani, K.; Tanaka, T. *J. Chem. Soc., Chem. Commun.* **1989**, 816–818.
- (28) (a) Islam, S. D. M.; Susdorf, T.; Penzkofer, A.; Hegemann, P. *Chem. Phys.* **2003**, *295*, 137–149. (b) Kowalczyk, R. M.; Schleicher, E.; Bittl, R.; Weber, S. *J. Am. Chem. Soc.* **2004**, *126*, 11393–11399. (c) Li, G.; Glusac, K. D. *J. Phys. Chem. A* **2008**, *112*, 4573–4583. (d) Quick, M.; Weigel, A.; Ernsting, N. P. *J. Phys. Chem. B* **2013**, *117*, 5441–5447.
- (29) Denney, D. B.; Klemchuk, P. P. *J. Am. Chem. Soc.* **1958**, *80*, 3289–3290.
- (30) (a) Kenner, G. W.; Murray, M. A.; Tylor, C. M. B. *Tetrahedron* **1957**, *1*, 259–268. (b) Coyle, J. C. *Chem. Rev.* **1978**, *78*, 97–123.
- (31) Costentin, C.; Robert, M.; Savéant, J.-M. *J. Am. Chem. Soc.* **2006**, *128*, 8726–8727.